

## THERMODYNAMIC QUANTITIES FOR PURE LIQUIDS AND THE APPLICABILITY OF THE ASYMPTOTIC LAWS NEAR THE CRITICAL POINT

A. V. VORONEL', V. G. GORBUNOVA, V. A. SMIRNOV, N. G. SHMAKOV, and V. V. SHCHEKOKHIKHINA

All-union Scientific Research Institute for Physico-technical and Radio-engineering Measurements

Submitted February 2, 1972

Zh. Eksp. Teor. Fiz. 63, 964-980 (September, 1972)

The results are given of experiments on the measurement of the densities of coexisting phases and of the specific heats  $C_V$  on several isochores for argon and ethane. Values are obtained for the critical indices  $\alpha$  and  $\beta$ . It is shown that the fundamental question determining the range of applicability of the scaling-theory formulas is the question of the choice of the order parameter in the liquid. With the appropriate choice of order parameter, the range of applicability of the power laws is extremely wide and encompasses almost the whole range of existence of matter in the liquid state.

### INTRODUCTION

DESPITE the large amount of experimental material<sup>[1-4]</sup>, the situation concerning the functional dependence of the specific heat  $C_V$  on the temperature and pressure near the liquid-vapor critical point of a pure substance is not completely clear. The values taken for the critical indices, sometimes even by the same authors, vary within extremely wide limits, exceeding the possible errors. Thus, e.g., in a paper of Edwards et al.<sup>[3]</sup>, the index  $\alpha = 0.06 \pm 0.02$  is given for xenon, and in another paper by the same authors<sup>[4]</sup>, the index  $\alpha = 0.125 \pm 0.02$  is given for carbon dioxide, the difference in the indices being connected not with the change of substance, but with a change of point of view. This happens mainly because the choice of the interval of the measurements of the argument over which the index is determined is arbitrary. Theoretically, this interval is bounded on two sides. In the region of large deviations from the critical point, fundamental doubts arise as to the applicability of the expressions of scaling theory (cf. e.g.,<sup>[5]</sup>) for the thermodynamic quantities, and in the region immediately adjacent to the critical point, distorting factors come into play<sup>[6]</sup>, placing the reliability of the experimental data in doubt. As a result, ambiguity of interpretation arises as a consequence of the different assumptions of authors about the range of applicability of the approximating laws.

In the course of our experiments, preliminary communications about which have been published<sup>[7,8]</sup>, we have accumulated material which makes it possible to come to more definite conclusions. The scaling-theory formulas have been found to be applicable in a much wider range than is usually assumed. Below we present experimental material on measurements of the specific heats and coexistence curves of argon and ethane; this material was obtained as the result of a certain improvement of technique<sup>[9]</sup> and thus improves considerably on the accuracy of our previous results<sup>[1,2,9]</sup>.

### MEASUREMENT TECHNIQUE

In the improvement of the accuracy of a calorimetric experiment<sup>[9]</sup> close to the critical point after minimization of the principal errors (heat losses by radiation, losses through the leads, instability in the control of the adiabatic regime), second-order effects acquire the paramount role; these are temperature gradients in the calorimeter, instability of the work done by the stirrer, oscillations in the temperature of the reference coils, etc.

The most important condition for a "pure" experiment in the critical region is uniformity of the properties of the system over the volume. A well known source of nonuniformity is the gravitational field. In the vicinity of the critical point, it leads to an uneven distribution of the density of the substance over the height of the calorimeter, i.e., to the so-called hydrostatic effect. To eliminate it, different methods of stirring the substance are applied.

Less attention is usually given to nonuniformity of the properties of the system caused by the presence of temperature gradients in the calorimeter. We must distinguish nonstationary and stationary temperature gradients. Nonstationary gradients arise inside a system studied in a heterogeneous state. They are caused by the difference between the times of establishment of equilibrium in each of the phases. For equivalent disturbances of the system, the magnitude of such a gradient depends on how close one is to the critical point. The appearance of stationary gradients is caused by nonuniformity of the external temperature field and, for a heterogeneous state of the system, by the difference between the heat-transfer rates for the phases. Gradients caused by a difference in the properties of the phases should decrease as the critical point is approached, i.e., as the thermodynamic properties of the phases become closer.

Nonstationary temperature gradients in the calorimeter lead to the violation of the adiabatic regime of the calorimeter before equilibrium is established in the system. This can be a source of important errors

in the measurement of the specific heat. Stirring reduces these gradients, but, apparently, does not reduce them to zero.

The presence of a stationary temperature gradient arising from imperfect control conditions leads to a stationary gradient of the density and of other parameters of state of the system over the height of the calorimeter. Taking into account the cubic form of the coexistence curve in the coordinates  $T$  and  $\rho$ <sup>[8]</sup>, we may expect that even small temperature gradients induce an appreciable density gradient.

In order to decrease the effect of the temperature gradients on the results of the specific-heat measurements, we surrounded the calorimeter with a copper casing. For this to be effective, it is necessary that the thermal resistance along the casing be less than between the casing and the calorimeter walls. In practice, this is always realized, since the thermal resistance of a steel-copper boundary is greater than that in the copper. In this case, nonstationary gradients arising in the system during the heating will not appear in the external casing, and, consequently, will not lead to disturbance of the adiabatic regime.

In our laboratory, calorimeters (Fig. 1) having a capillary for filling have usually been used for investigating specific heats of liquids. The experimental error in this case is proportional to the volume of the capillary; for argon it amounts to 0.5%. However, if the working range of temperature is not far from room temperature, the capillary can be eliminated altogether by means of a locking valve, positioned directly on the calorimeter (Fig. 2). For this, we specially constructed a needle valve which, after locking, was disassembled without breaking the airtight seal of the calorimeter. The whole valve weighs 60 g, but the parts remaining in the calorimeter weight 6.5 g<sup>[10]</sup>.

In our calorimeters there is a differential thermocouple, the junction of which is attached to the top and bottom of the calorimeter to monitor the temperature gradient in this most hazardous direction. In our previous experiments<sup>[2,9]</sup>, the maximum value of the temperature difference was kept less than a calorimetric step and amounted to 0.01°. As a result of all the measures taken, the temperature gradients over the height of the calorimeter were reduced by more than an order of magnitude. This led also to a decrease of the time of establishment of equilibrium in the calorimetric system and increased the accuracy of the measurements.

Much attention was given to the stirring of the substance during the experiment. In the calorimeter depicted in Fig. 1, we used a magnetic stirrer which performs rotational-translational motion along the vertical axis of the calorimeter. The motion of the stirrer was induced by automatic switching of the current in coils creating a magnetic field at the various levels and corresponding to the bottom and top of the calorimeter. As the investigation has shown, the work of the stirrer introduces additional heat fluxes, which are easily compensated by the difference in temperature between the plates and the calorimeter. It is very important that these heat fluxes be constant, and this is determined by the stability of the sources in the chain of solenoids. Storage cells served as these sources. The frequency

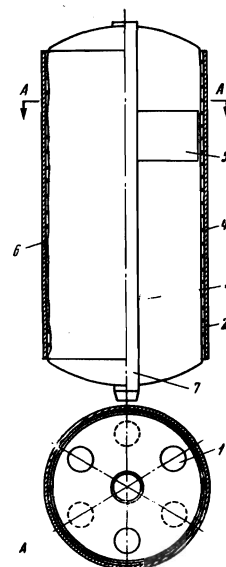


FIG. 1. Construction of the calorimeter: 1—aperture in the magnetic stirrer, 2—gap between the calorimeter and the copper cylinder, 3—calorimeter wall, 4—calorimeter heater, 5—magnetic stirrer, 6—copper cylinder playing the role of an isothermal casing, 7—platinum resistance thermometer.

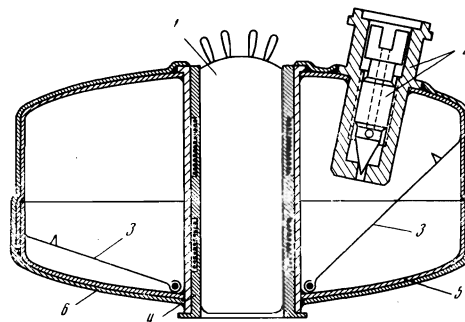


FIG. 2. Calorimeter with isothermal casing. 1—platinum resistance thermometer, 2—valve seat and needle, 3—stirrer platelets, 4—heater unit, 5—body of the calorimeter, 6—copper casing.

of the stirring and the speed of the stirrer determine how rapidly one can reach equilibrium and a uniform state of matter in the system. The necessary stirring frequency was determined experimentally. The duration of one cycle was 20 sec.

When the currents are switched on or off, stray emf's appear in the circuit of coils in the thermocouple detectors; these are proportional to the rate of change of the magnetic flux and to the area of the thermocouple circuit. Although a double-wound coil decreases the magnitude of this area, it does not seem possible to reduce it to zero. To compensate this, an additional loop, connected in opposition, is attached in series to the thermocouple circuit, from the outside, on the level of the magnetic coils. The sum of the stray emf's in the compensating loop and in the thermocouple circuit positioned inside the apparatus must be equal to zero.

In the calorimeter shown in Fig. 2, the stirring is effected by the rotation of four platelets of area 3–4 cm<sup>2</sup> about four horizontal axes at the bottom of the calorimeter. The platelets are displaced through an angle of 70–75° and are set in motion by the magnetic field of a solenoid. Because of the increase in accuracy, we have succeeded in measuring the specific heats of argon and ethane near the critical point with a

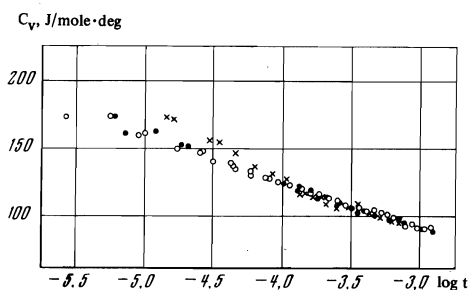


FIG. 3. Specific heat of ethane near the critical point for different stirrings ( $T > T_c$ ). X—for 4 stirrings per minute,  $I_{\text{solenoid}} = 2.5$  a, O— for 4 stirrings per minute,  $I_{\text{solenoid}} = 1.5$  a, ●—for 6 stirrings per minute,  $I_{\text{solenoid}} = 4$  a.

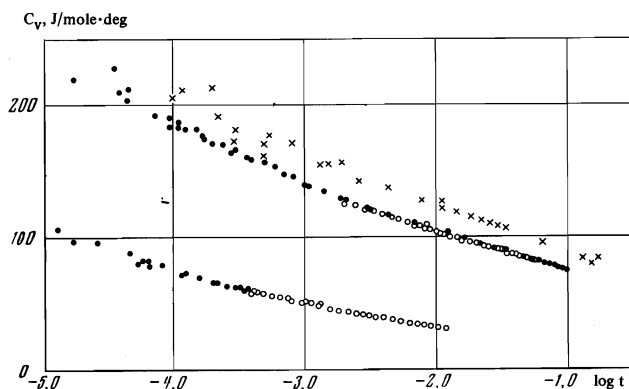


FIG. 4. Specific heat of argon  $C_V = f(\log t)$ . The upper curve corresponds to  $T < T_c$  and the lower to  $T > T_c$ . ●—with stirring, ○—without stirring, X—specific heat of nitrogen,  $T < T_c$  [1].

precision approximately an order greater than in the previous work<sup>[1,2]</sup>.

The question of the hydrostatic effect and of the role of stirring is extremely difficult and is not a matter only of technique. In the work of Edwards et al.<sup>[3]</sup>, the hydrostatic effect essentially determined the results, and in our work<sup>[1,2]</sup> also evidently played a not unimportant role. As was shown by Berestov and Malyshenko<sup>[11]</sup>, stirring does not completely eliminate the gravitational effect; therefore, the interpretation of the results partly depends on the information about the hydrostatic effect available to the experimenter. Our latest experiment tells us that up to approximately  $t \sim 10^{-3} - 10^{-4}$  the hydrostatic effect either does not appear at all or is manifested only in a slowing down of the establishment of equilibrium, which is easily eliminated by stirring. However, on closer approach to the critical point, a noticeable dependence of the results on the intensity and frequency of the stirring arises (Fig. 3). Since it is extremely difficult to select the optimum stirring that would only compensate the hydrostatic effect and would not introduce additional effects, we have preferred, in studying the form of the dependence of  $C_V$  on  $t$ , to exclude from consideration the whole of the region  $|t| < 10^{-4}$  sensitive to stirring and subject to the influence of the hydrostatic effect. The results of our previous paper<sup>[12]</sup> devoted to this question were evidently strongly distorted by the influence of the temperature gradient, which acts like a density

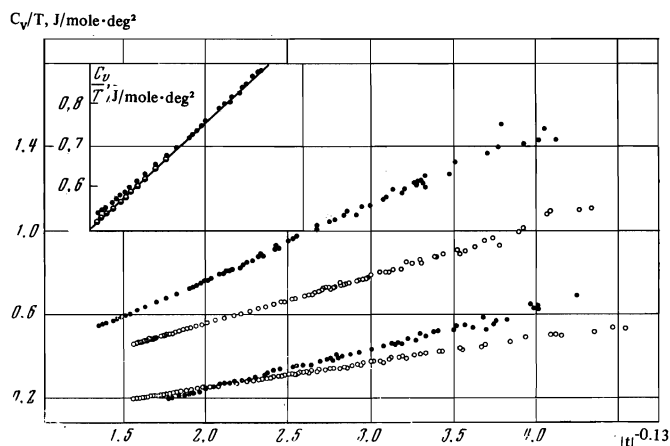


FIG. 5. Dependence of  $C_V/T$  on  $t^{-0.13}$  for argon and ethane. ●— $C_V$  of argon, ○— $C_V$  of ethane, ●— $C_{VD}$  of argon; the continuous line in the upper left corner corresponds to formula (2).

gradient<sup>[11]</sup>. Therefore, although the results of<sup>[12]</sup> are qualitatively confirmed, all the quantitative estimates must be revised. Only after we have eliminated temperature gradients in the calorimeter (Fig. 2) can we pose the question of the detection of true hydrostatic effects. The establishment of equilibrium without stirring in such conditions takes up to ten hours. This means that we have not been able up to now to accumulate sufficiently representative material to compare it quantitatively with the existing theory<sup>[13]</sup>.

In measuring these points, especially those near  $T_c$ , in ethane, we have succeeded in observing the effect, predicted by Giterman and Shteinberg<sup>[14]</sup>, of the nonlinear equilization of temperature under conditions when the hydrostatic effect is operative. It appears in a pronounced paradoxical underestimate of the time of equilization on increase of the temperature disturbance.

In aggregate, the measures taken ensured us a precision in the measurement of the specific heats of argon and ethane almost an order greater than in the previous works<sup>[1,2,9]</sup>. In Figs. 4 and 5, our data are plotted on semi-logarithmic and power scales. The approximateness of our previous idea<sup>[1,2]</sup> about the logarithmic nature of the specific-heat singularity in the vicinity of the critical point can be clearly seen.

## THE ARGON COEXISTENCE CURVE

Although the specific-heat measurements in the adiabatic calorimeter are characterized by high precision, they are comparatively roughly linked to the temperature scale. The specific-heat coordinate of a point can be determined only with a precision not greater than the width of the calorimetric step  $\Delta T$ , because of the differential nature of the actual quantity  $C = \Delta Q/\Delta T$ . However, for sufficiently reliable adiabaticity, one can propose an integral technique for the heat measurements, which distinguishes the singular points on the thermodynamic surfaces with a precision better than  $0.001^\circ$  (in the best experiments in the calorimeter of Fig. 2, it was possible to reproduce a stable critical temperature of ethane with an even greater precision of  $\sim 0.0001^\circ$ ). The technique of

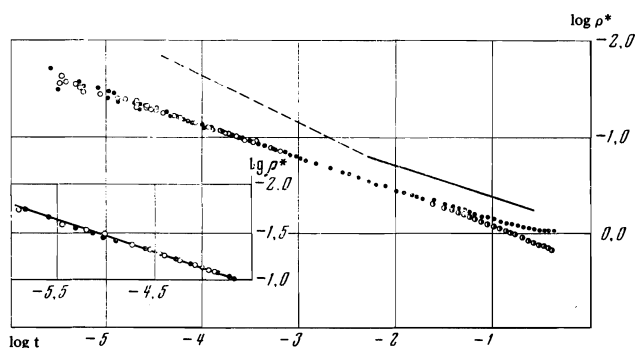


FIG. 6. Coexistence curve for argon.  $\circ$ — $\rho < \rho_c$ ;  $\bullet$ — $\rho > \rho_c$ ; the continuous line corresponds to a slope  $\beta = 1/3$ , and the dashed line to a slope  $\beta = 1/2$ ;  $\rho^* = |\rho - \rho_c|/\rho_c$ .

quasi-static thermograms, already described in part previously<sup>[8,9]</sup>, is such a technique.

The substance in the adiabatic calorimeter is slowly heated (or cooled) at constant density with stirring, with a constant temperature difference  $\delta T$  between the calorimeter and the adiabatic screen. In a narrow range of temperatures, constancy of  $\delta T$  implies constancy of the heat intake, and the energy of the system can thus be assumed to be a linear function of time. Then the time dependence of the temperature of the system will represent, on an arbitrary scale, the functional relation between the temperature and energy. At the point where the system changes state, this curve contains a break, which is connected mainly with the presence of a jump in the specific heat and could be detected easily on the graph with a precision of  $\sim 2 \times 10^{-4}$  (cf.<sup>[11]</sup>). By performing several such heatings and coolings at the same density and averaging the results, we obtain the temperature of the singular point with a precision better than  $1 \times 10^{-3}$ . The rate of change of temperature in the heating and cooling should be such that the state of the substance at each given time can be assumed to be an equilibrium state. Our previous determinations of the times of establishment of equilibrium enable us to estimate a lower bound for the equilibrium rate at various distances from the critical point. A large part of the results on the coexistence curves of argon was obtained with rates of  $\sim (2-3) \times 10^{-5}$  deg/min. This rate is at least an order slower than the rate with which experimenters usually approach the stratification point of a system<sup>[15,16]</sup>, and guarantees us a reliable approach to the critical point up to  $t \sim 10^{-5}$ . In the region from  $t = 10^{-4}$  to  $t = 10^{-6}$ , the scatter of the points relative to the approximating curve (Fig. 6) gradually increases, which we interpret as an increase of the extent of nonequilibrium. Indeed, a decrease of the rate to  $\sim 5 \times 10^{-6}$  deg/min noticeably increases the reproducibility of the points in this region (Fig. 6, inset). However, it still does not follow from the good applicability of the same dependence in both the region  $t \sim 10^{-2}-10^{-4}$  and the region  $t \sim 10^{-5}-10^{-6}$  that it is correct for  $t < 10^{-4}$ . The applicability was attained as the result of an appropriate choice of  $T_c$ . The value we chose was  $T_c = 150.663_3^\circ\text{K}$ , whereas the scatter of the points permits a choice from  $150.663$  to  $150.663_5^\circ\text{K}$ . We shall examine this question in more detail.

In the measurements of the coexistence curve of ethane in 1967<sup>[17]</sup>, the calorimeter did not have all the improvements described in the preceding section. Therefore, as in<sup>[2]</sup>, the existence of additional maxima in the temperature dependence of the specific heat was detected in the thermograms; this was successfully explained<sup>[11]</sup> by the influence of inhomogeneities in the temperature and density of the substance along the calorimeter.

Owing, apparently, to the improvement in the stirring, we detected no traces of these maxima when measuring the coexistence curve of argon. This means that the possible temperature gradient in these latest experiments is less than  $3 \times 10^{-3}$ . This number in fact also determines the possible limits on the choice of  $T_c$ . The effective height characterizing the inhomogeneity of the substance is in this case less than 0.05 cm. In the subsequent specific heat measurements, because of the equalizing copper jacket (see Figs. 1 and 2), the uniformity of the temperature and, correspondingly, of the state of the substance over the height of the calorimeter was found to be several times higher still, and the choice of  $T_c$  was narrowed to  $0.001^\circ$ . We note that the determination of the value of the critical temperature on the thermometer's own scale differs somewhat from the determination of the temperature on the thermodynamic scale. The latter cannot be achieved more accurately than by  $\pm 0.01^\circ$ , and this leads to some possible disagreement between different experiments. The data on the coexistence curve of argon are given in Table I and in Fig. 6. In the range of temperatures  $t = 10^{-2} - 5 \times 10^{-6}$  and

Table I. Phase density as a function of temperature on the coexistence curve

$\rho, \text{g/cm}^3$	$T, ^\circ\text{K}$	$\rho, \text{g/cm}^3$	$T, ^\circ\text{K}$	$\rho, \text{g/cm}^3$	$T, ^\circ\text{K}$
Series I					
0.7690	147.843	0.5906	150.5960	0.5698	150.6484
0.7566	148.213	0.5906	150.6127	0.5661	150.6521
				0.5624	150.6553
0.7443	148.450	0.5851	150.6237	0.5587	150.6578
0.7209	149.128	0.5813	150.6318	0.5549	150.6594
0.7033	149.484	0.5776	150.6383	0.5512	150.6614
0.6916	149.695	0.5727	150.6470	0.5493	150.6619
0.6800	149.875	0.5688	150.6510	0.5475	150.6622
0.6686	150.036	0.5632	150.6559	0.5456	150.6626
0.6569	150.172	0.5576	150.6593	0.5438	150.6628
0.6511	150.233	0.5540	150.6616	0.5419	150.6629
0.6394	150.341	0.5521	150.6620	0.5401	150.6631
0.6162	150.504	0.5493	150.6633	0.5383	150.6632
0.7326	148.846	0.5146	150.6627	0.5372	150.6632
		0.5110	150.6612	0.5364	150.6634
Series II					
0.5198	150.6530	0.5049	150.6587	0.5355	150.6632
0.5174	150.6626	0.4987	150.6545	0.5345	150.6635
0.5148	150.6624	0.4913	150.6470	0.5340	150.6634
0.5110	150.6608	0.4840	150.6344	0.5330	150.6634
0.5071	150.6595	0.4766	150.6222	0.5320	150.6632
0.5031	150.6572	Series IV			
0.4992	150.6545	0.5746	150.6434	0.5311	150.6633
0.4946	150.6502	0.5709	150.6478	0.5301	150.6635
0.4903	150.6450	0.5671	150.6519	0.5292	150.6634
0.4855	150.6370	0.5634	150.6553	0.5283	150.6633
0.4802	150.6279	0.5597	150.6581	0.5273	150.6634
0.4745	150.6150	0.5592	150.6598	0.5264	150.6632
0.4669	150.5940	0.5522	150.6616	0.5255	150.6631
0.4594	150.5666	0.5485	150.6628	0.5245	150.6632
0.5543	150.6612	0.5447	150.6633	0.5225	150.6631
0.5519	150.6624	0.5267	150.6634	0.5207	150.6631
0.5496	150.6630	0.5240	150.6632	0.5188	150.6628
Series III					
0.5163	150.6624	0.5221	150.6630	0.5170	150.6628
0.6223	150.4800	0.5202	150.6628	0.5149	150.6624
0.6150	150.5190	0.5182	150.6627	0.5130	150.6619
0.6114	150.5380	0.5144	150.6621	0.5093	150.6604
0.6076	150.5525	0.5067	150.6600	0.5055	150.6590
0.6021	150.5753	Series V			
		0.5810	150.6312	0.5017	150.6572
		0.5792	150.6344	0.4978	150.6546
		0.5736	150.6433	0.4941	150.6509
				0.4903	150.6465
				0.4866	150.6416

Table II. Specific heat of argon for population density  $\rho = 0.531_2 \text{ g/cm}^3$

$T_1$ , °K	$T_2$ , °K*	J/mole-deg	$T_1$ , °K	$T_2$ , °K*	J/mole-deg
135.315	135.872	73.6	150.5963	150.6166	158.8
135.864	136.416	74.0	150.6166	150.6362	168.3
136.414	136.962	74.5	150.6362	150.6453	179.8
136.960	138.042	75.5	150.6451	150.6616	202.4
138.036	139.099	76.7	150.6676	150.6864	80.0
139.094	140.140	78.1	150.6335	150.6430	174.5
140.129	141.158	79.6	150.6428	150.6525	185.5
141.146	142.159	80.7	150.6522	150.6635	223.5
142.151	143.145	82.4	150.6668	150.6823	82.3
143.138	144.115	84.0	150.6797	150.7012	69.0
144.102	145.060	85.8	150.6349	150.6506	178.6
145.050	145.988	88.0	150.6506	150.6631	212.0
145.974	146.890	90.6	150.6673	150.6812	77.7
146.878	147.770	93.6	150.6824	150.7049	67.7
147.756	148.618	97.4	150.7057	150.7418	61.5
148.603	149.021	101.1	150.6411	150.6541	186.0
149.0015	149.4045	104.2	150.6523	150.6637	215.1
149.3980	149.7920	108.4	150.6448	150.6584	199.0
149.7672	150.1442	114.5	150.6669	150.6800	84.7
150.1342	150.2550	120.5	150.6804	150.6956	69.1
150.2469	150.4211	126.0	150.6944	150.7134	64.5
150.4077	150.5697	137.8	150.6660	150.6736	93.8
150.5582	150.6475	162.2	150.6735	150.6823	77.1
150.6358	150.6602	190.6	150.6816	150.6910	69.6
150.6718	150.7062	71.0	150.6669	150.6759	85.3
150.7035	150.7425	59.6	150.6747	150.6855	74.6
150.6524	150.6616	174.3	150.6659	150.6728	93.2
149.9960	150.3168	119.6	150.6726	150.6848	77.7
150.3168	150.4181	127.6	150.6660	150.6744	93.2
150.4181	150.4714	132.7	149.6109	149.7113	108.9
150.4710	150.5230	136.9	149.7112	149.8104	110.4
150.5231	150.5480	143.6	149.8101	149.9080	112.0
150.5476	150.5640	146.5	149.9020	150.0042	114.5
150.5634	150.5794	152.0	150.0042	150.0990	116.2
150.5790	150.5948	154.4	150.0990	150.1919	119.2
150.5934	150.6088	157.3	150.1919	150.2833	121.5
150.6093	150.6242	164.6	150.2190	150.3085	122.5
150.6249	150.6394	169.4	150.3077	150.3952	125.9
150.6395	150.6530	184.7	150.3945	150.4787	131.7
150.6543	150.6616	226.9	150.4773	150.5573	140.0
150.6534	150.6639	218.9	150.5570	150.6303	155.6
150.6299	150.6441	173.4	150.6299	150.6611	137.5
150.6438	150.6543	189.3	149.9057	150.6571	128.7
150.6539	150.6599	210.7	150.2989	150.3624	123.8
150.6594	150.6646	244.6	150.3624	150.4488	128.9
150.6691	150.6812	81.8	150.4231	150.4734	133.0
150.6826	150.6961	69.2	150.4740	150.5228	138.0
150.6966	150.7110	63.2	150.5235	150.5625	144.2
150.6666	150.6719	96.2	150.5634	150.6049	151.4
150.6717	150.6779	78.8	150.6054	150.6632	179.3
150.6771	150.6917	72.2	150.6060	150.6606	176.0
150.6909	150.7035	65.6			
150.6654	150.6687	106.1			
150.6656	150.6704	96.2			
150.6691	150.6747	87.1			
150.6700	150.6820	82.0			
150.6716	150.6868	78.1			
150.5961	150.6293	162.0			
150.6286	150.6586	182.0			
150.6379	150.6508	180.2			
150.6506	150.6620	209.1			
150.6311	150.6559	183.7			
150.6303	150.6561	181.6			
145.4257	145.8763	88.2			
145.8766	146.0154	89.5			
146.0176	146.1564	89.8			
146.1549	146.2931	90.3			
146.2941	146.4319	90.7			
146.4318	146.7962	91.4			
146.7957	147.1563	92.4			
147.1579	147.5141	93.7			
147.5141	147.8659	95.1			
147.8662	148.2138	96.6			
148.2135	148.4605	97.9			
148.4587	148.7033	99.2			
148.7016	148.9424	101.1			
148.9430	149.1890	102.6			
149.0470	149.2050	103.8			
149.2065	149.3595	107.6			
149.3589	149.5131	106.4			
149.5142	149.6658	108.4			
149.4345	149.5875	107.5			
149.6734	149.7246	109.0			
149.7200	149.8680	111.7			
149.8518	149.9562	112.8			
149.9525	150.0555	114.8			
150.0497	150.1503	118.3			
150.1466	150.2214	119.2			
150.2143	150.2877	122.2			
150.2818	150.3542	123.9			
150.4110	150.4810	129.0			
150.4720	150.5400	134.6			
150.5298	150.5942	143.6			
148.7743	149.0197	101.3			
149.0062	149.1098	102.3			
149.1059	149.2101	103.5			
149.1975	149.2985	105.2			

$T_1$ , °K	$T_2$ , °K*	J/mole-deg	$T_1$ , °K	$T_2$ , °K*	J/mole-deg
149.2888	149.3392	105.2			
149.3328	149.3832	105.3			
150.6828	150.7152	65.4			
150.7155	150.7505	58.1			
150.7360	150.7600	61.0			
150.7606	150.7994	53.4			
150.7998	150.8402	50.4			
150.8412	150.8828	48.0			
150.8824	150.9256	45.1			
150.9250	150.9670	43.9			

\* $T_1$  and  $T_2$  are the temperatures at the beginning and end of the calorimetric experiment.

densities  $\rho^* = |\rho - \rho_C|/\rho_C = (0.5-2) \times 10^{-2}$ , the coexistence curve is expressed by the formula

$$\rho^* = k t^\beta \tag{1}$$

with the constants  $\beta = 0.34 \pm 0.02$ ,  $k = 1.6 \pm 0.1$ ,  $\rho_C = 0.531_0 \text{ g/cm}^3$  and  $T_C = 150.663_3^\circ\text{K}$ .

### SPECIFIC HEAT OF ARGON AND ETHANE AT THE CRITICAL DENSITY

The specific heat of argon at density  $\rho = 0.531_2 \text{ g/cm}^3$  was measured in the calorimeter of Fig. 1, and the specific heat of ethane at density  $\rho = 0.204_1 \text{ g/cm}^3$  was measured in the calorimeter of Fig. 2. The numerical data for argon are given in Table II and in Fig. 5. The curves were approximated by the formula

$$\frac{C_v}{T} = A_\pm |t|^{-\alpha} + B_\pm, \tag{2}$$

where  $A_+$  and  $B_+$  correspond to  $t > 0$ , and  $A_-$  and  $B_-$  correspond to  $t < 0$ .

The constants were determined by the least-squares method with a computer; this reduced to the minimization of the expression

$$\sum_{i=1}^n \left[ \left( \frac{C_v}{T} \right)_{\text{exp}}^i - \frac{T_C A}{\Delta T_i (1-\alpha)} [t_{2i}^{1-\alpha} - t_{1i}^{1-\alpha}] - B \right]^2 \left[ \left( \frac{C_v}{T} \right)_{\text{exp}}^i \right]^{-2}$$

where  $C_v^i$  exp was equated to

$$\frac{1}{\Delta T_i} \int_{T_{1i}}^{T_{2i}} C_v dT$$

and referred to

$$t_i = \left\{ \frac{T_C}{\Delta T_i (1-\alpha)} [t_{2i}^{1-\alpha} - t_{1i}^{1-\alpha}] \right\}^{-1/\alpha}$$

The value of  $\alpha$  was chosen from the condition that the sum of the squares of the errors in the given interval of  $t$  be a minimum. As already remarked, the accuracy of our previous work did not permit us to distinguish the index  $\alpha$  reliably from zero within the limits 0–0.2. In the present work, we can sharply narrow the range of possible values of  $\alpha$ . Figures 7a and 7b characterize the precision of the measurements and show that the most probable values of  $\alpha$  for argon and ethane lie in the vicinity of  $\alpha = 1/3$ . The differences between the curves of Figs. 7a and 7b are more likely to be characteristic of a systematic difference between the experiments in the calorimeters of Fig. 1 and Fig. 2 than of a difference in the properties of argon and ethane. Nevertheless, it is not excluded that the true value of  $\alpha$  will turn out to be somewhat greater than

Table III. Values of the constants of Eq. (2) for different  $\alpha$  and  $T_c$

	$\alpha$	Argon				Ethane			
		$T'_c = 150.663, ^\circ\text{K}$		$T'_c = 150.664, ^\circ\text{K}$		$T'_c = 305.362, ^\circ\text{K}$		$T'_c = 305.363, ^\circ\text{K}$	
		A	B	A	B	A	B	A	B
$T < T_K$	0.11	0.504	-0.151	0.519	-0.179	0.301	0.016	0.303	0.012
	0.12	0.429	-0.058	0.442	-0.084	0.257	0.069	0.259	0.065
	0.13	0.368	0.021	0.380	-0.003	0.221	0.113	0.223	0.109
	0.14	0.317	0.089	0.328	0.066	0.192	0.152	0.193	0.148
	0.15	0.275	0.147	0.284	0.126	0.167	0.185	0.168	0.181
	0.16	0.239	0.198	0.247	0.178	0.146	0.214	0.147	0.210
$T > T_K$	0.11	0.275	-0.252	0.270	-0.243	0.166	-0.052	0.165	-0.050
	0.12	0.235	-0.204	0.231	-0.196	0.142	-0.022	0.141	-0.020
	0.13	0.203	-0.164	0.199	-0.156	0.123	0.003	0.125	0.005
	0.14	0.176	-0.129	0.173	-0.122	0.106	0.024	0.105	0.026
	0.15	0.153	-0.100	0.150	-0.093	0.092	0.043	0.092	0.045
	0.16	0.134	-0.074	0.131	-0.067	0.081	0.060	0.080	0.061

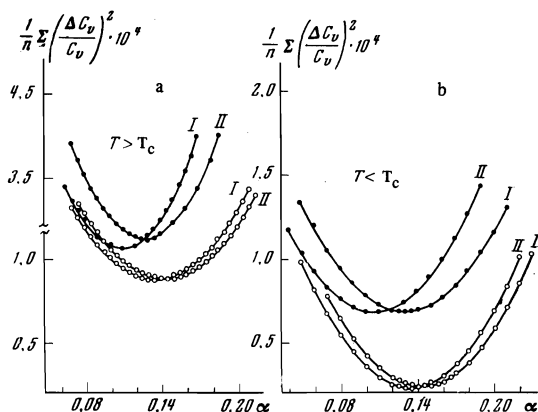


FIG. 7. The mean square relative deviation from the approximating curve  $C_V/T = A_{\pm}t^{\alpha} + B_{\pm}$  as a function of  $\alpha$ . a— $T > T_c$ , b— $T < T_c$ .  $\circ$ —argon,  $\circ$ —ethane; for argon: I— $T'_c = 150.664, ^\circ\text{K}$ , II— $T''_c = 150.663, ^\circ\text{K}$ ; for ethane: I— $T'_c = 305.363, ^\circ\text{K}$ , II— $T''_c = 305.362, ^\circ\text{K}$ .

$1/8$  since the experiment with ethane seems to us to be the more perfected.

The values of  $T_c$  for argon and ethane were chosen from the thermograms (cf. the preceding Section) independently of the measurements of  $C_V$ , and the most probable values (on the thermometer's own scale, of course) appear to be  $T_c = 150.664, ^\circ\text{K}$  for argon and  $T_c = 305.362, ^\circ\text{K}$  for ethane. In Figs. 7a and 7b, it can be seen how the choice of  $T_c$  within the permitted limits affects the value of  $\alpha$ . The values of  $A_{\pm}$  and  $B_{\pm}$  for different  $\alpha$  were selected over the interval from  $t = 10^{-2}$  to  $t = 10^{-4}$ . The results of this matching are given in Table III.

#### THE SPECIFIC HEAT OF ARGON FOR $\rho \neq \rho_c$ AND CALCULATION OF THE THERMODYNAMIC QUANTITIES ON THE COEXISTENCE CURVE

For argon the specific heat was measured again, for several non-critical densities. The difference from the old results<sup>[2]</sup> reduced mainly to the disappearance of the additional maxima in the heterogeneous region, which, as we now know<sup>[11]</sup>, arise as a result of non-uniformity of the state of the substance in the vessel. However, our results agree qualitatively with the previous results. Thus, the dependence  $C_V(\rho)$  obtained

in the present work turned out to correspond to the scaling theory<sup>[7]</sup>:

$$C_v/T \sim D|\rho|^{\epsilon}. \quad (3)$$

The values of the constants are  $\epsilon = 0.35 \pm 0.04$  and  $D = 0.15 \pm 0.02$ . Treatment of our old material<sup>[2]</sup> using formula (3) gives  $\epsilon = 0.34 \pm 0.15$ , which can be considered to be satisfactory agreement. As in the case of the dependence  $C_V(T)$  (see the preceding Section), the greater accuracy of the formula is the result of an increase in the precision of the measurements, but in the present case there is also, in addition, the constancy of the composition of the argon sample (the quantity of impurities in our sample now is less than 0.01% whilst in our old samples<sup>[2]</sup> this quantity varied from 0.6 to 0.1% in the various experiments).

The data were obtained at densities of 0.692<sub>g</sub>, 0.522<sub>g</sub>, 0.515<sub>g</sub>, 0.511<sub>g</sub>, 0.496<sub>g</sub> and 0.295<sub>g</sub>  $\text{g}/\text{cm}^3$ . In the region of the two-phase state, for the density dependence of the specific heat we have the formula<sup>[18]</sup>:

$$\frac{C_v}{T} = V \frac{d^2p}{dT^2} - \frac{d^2\mu}{dT^2}. \quad (4)$$

Here  $V = M/\rho$  is the average molecular volume of the whole system, and  $p$  and  $\mu$  are the pressure and chemical potential of a phase on the coexistence curve. By making use of the fact that we have experimental data for several (at least two) densities, we can obtain functional expressions for both terms of this formula;

$$\frac{d^2p}{dT^2} = \frac{C_{v1} - C_{v2}}{T(V_1 - V_2)}, \quad \frac{d^2\mu}{dT^2} = \frac{V_2 C_{v1} - V_1 C_{v2}}{T(V_1 - V_2)}, \quad (5)$$

where  $V_1 = M/\rho_1$  and  $V_2 = M/\rho_2$ . In Fig. 8, the results of a calculation of these quantities from our experimental data are shown. It can be seen that the quantity  $d^2p/dT^2$ , like  $C_V$ , has a singularity, as we assumed previously<sup>[19]</sup>. The derivative  $d^2\mu/dT^2$ , on the other hand, looks like a smooth function, confirming, perhaps, the correctness of the assumption at the basis of the theory of the equation of state<sup>[20]</sup>.

#### DISCUSSION OF THE RESULTS

In analyzing the experimental data and attempting to interpret them on the basis of the scaling theory, we encounter difficulties arising from the indeterminacy of the interval in which this theory should be fulfilled. In principle, the expressions of the theory are

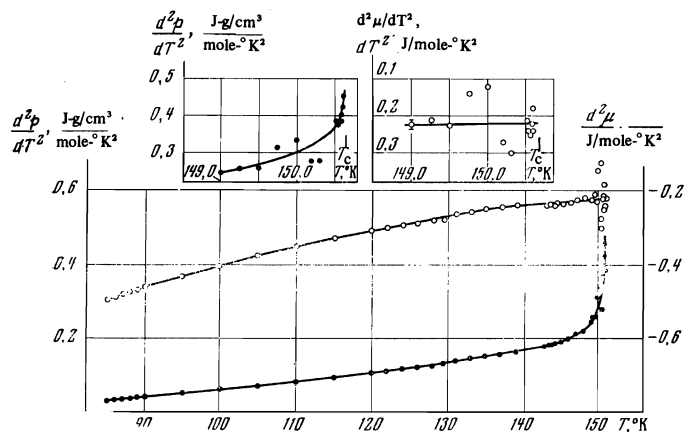


FIG. 8. ●—dependence of  $d^2p/dT^2$  on  $T$  for argon (scale on the left), ○—dependence of  $d^2\mu/dT^2$  on  $T$  for argon (scale on the right). The upper curves are the same, on an expanded temperature scale.

asymptotic and should be fulfilled only in the limit of very small  $t$ . Experiment, however, is limited in advance both by technique and by the state of the sample, which usually stringently limit the approach to  $T_C$ . For example, up to the present time there has not been one reliable experiment with a solid which would give the possibility of using an approach closer than  $t = 10^{-3}$  [6]. This is connected with the fact that in solid samples we cannot get rid of the intrinsic defects of the structure.

In work with liquid samples, the asymptotic dependences have been observed ostensibly to  $t \sim 10^{-6} - 10^{-7}$  [21,22]; however, we do not have complete confidence that the experimental conditions in all cases do not distort the sample at such close approaches to  $T_C$ . In the second Section we have already remarked that in interpreting the data we can consider only the closeness  $t \sim 10^{-4}$  to be absolutely reliable. The region between  $10^{-4}$  and  $10^{-5}$  depends on our view of the role of the gravitational effect and on the correctness of our estimate of the effect of stirring.

With the existing limited accuracy, it is only possible to judge reliably about the form of the dependences, and thereby about the critical indices, if we have a sufficiently broad interval over which the approach to  $T_C$  is made. Therefore, it is especially important to know the maximum  $t$  up to which the formulas of the scaling theory can be assumed to be applicable. We have at our disposal no quantitative estimate, apart from  $t \ll 1$  [5]. We write down the expression for the free energy in the scaling theory:

$$F = t^{2-\alpha} f\left(\frac{\eta}{t^\beta}\right) + F_0(\rho, t), \quad (6)$$

where  $\eta$  is the order parameter, depending on the population density  $\rho$ . It is clear that, in addition to the second approximation, the form of the functions  $f(\eta/t^\beta)$  and  $F_0$  and of their derivatives will also affect the range of applicability of the simple power dependences. Although it is by no means clear in advance to what extent these are complicated functions of their arguments, we shall start from the assumption that, for the correct choice of order parameter  $\eta$ , the form of the function  $f$  will be of maximum simplicity.

We remark that, at the present time, the choice of

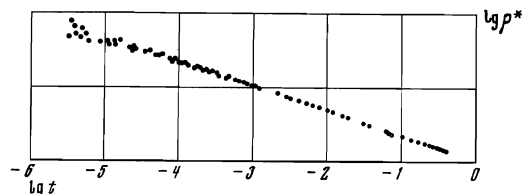


FIG. 9. Coexistence curve of argon in the coordinates  $\log[(\rho_{\text{liq}} - \rho_{\text{vap}})/\rho_0] \sim \log t$ .

the order parameter in practice is not based on any physical considerations, but is dictated to us by the experimental situation. The very idea of the existence of an order parameter at a phase-transition point is connected with the concept of some kind of isomorphism of all systems in the neighborhood of the phase transition. Obviously, the isomorphous quantity  $\eta$  in the different systems can be a different function of the experimentally measured quantities [23]. We can assume that the most correct choice will be that giving the maximum range of applicability of the scaling-theory formulas.

In Fig. 6 can be seen the applicability of formula (1) corresponding to the order parameter defined as  $\eta = \rho^* = |(\rho - \rho_C)/\rho_C|$ . Incidentally, by defining this parameter as  $\eta = (\rho - \rho_D)/\rho_0$ , where  $\rho_D = (\rho_1 + \rho_V)/2$  and  $\rho_0$  is determined from the extrapolation of  $2\rho_D$  to  $0^\circ\text{K}$ , we have discovered a substantial broadening of the range of applicability of formula (1), since in this case  $\rho^* = (\rho_1 - \rho_V)/\rho_0$  (cf. Fig. 9). Whereas with the first definition of the parameter  $\eta$ , a deviation of the average population density  $\rho$  from  $\rho_C$  corresponded to the presence of a non-zero field  $H$ , and  $CH_{=0} = C_{V_C}$ , in the second case the definition of  $CH_{=0}$  is more complicated and corresponds to  $C_{V_D}$  or  $C_V$ , the isochore (or ordinary) specific heat, defined along the so-called "rectilinear" diameter. Thus, it is possible that the correct thermodynamic path for the definition of the singular specific heat  $CH_{=0}$  is the line of the "rectilinear" diameter, which, generally speaking, can itself be singular [24].

We note that, for a liquid, the parameter that is completely analogous to  $(N_1 - N_2)/N$  in the Ising model, where  $N_1$  and  $N_2$  are the numbers of spins in opposite directions, will be the parameter

$$\eta = \frac{\rho(\rho_{\text{liq}} + \rho_{\text{vap}}) - 2\rho_{\text{liq}}\rho_{\text{vap}}}{\rho(\rho_{\text{liq}} - \rho_{\text{vap}})}$$

The case  $H = 0$  is realized when the population density  $\rho$  is equal to  $\rho_C$ . However, to introduce the right corrections and realize the path of  $CH_{=0}$  is even more difficult in this case. The index  $\beta$  can also depend essentially on the choice of this parameter. For example, for argon, this index can vary from 0.3 to 0.38 depending on the choice of  $\eta$ .

In the treatment of the data of Edwards et al. [3,4], it was clear that even  $t \sim 10^{-2} - 10^{-3}$  is still not small enough to determine the form of the singularity. This is connected also with the neglect of the smooth temperature dependence obtained from the differentiation of formula (6). From the scaling theory, the equality for the specific heat that arises from (6) should have the form of (2). With experimental accuracy of  $\sim 0.1\%$ , the deviation of  $T$  from  $T_C$  will be important up to

$t \sim 10^{-3}$ . Allowance for this correction gives applicability of the power formula up to  $t \sim 10^{-2}$  (see the upper left corner of Fig. 5).

The fact that  $E_+$  and  $B_-$  are not equal requires attention. Since the scaling-theory expressions are symmetric with respect to the sign of  $t$ , for the correct thermodynamic path ( $H = 0$ )  $B_+$  and  $B_-$  ought to be equal (disregarding the second approximation). The absence of equality (also observed in the work of Edwards et al.<sup>[3,4]</sup>) may mean that the path  $\rho = \rho_C$  does not coincide with  $H = 0$ . We note also that the definition of the path  $H = 0$ , generally speaking, can be different above and below  $T_C$ , so that a line which is continuous in the coordinates  $\eta - T$  may have a break in the coordinates  $\rho - T$ . Thus, if we choose the path

$$C_{H=0} = \begin{cases} C_d(T < T_C) \\ C_{vc}(T > T_C) \end{cases},$$

we can achieve equality of  $B_-$  and  $B_+$  in formula (2). Then  $A_-$  changes, and it turns out that  $A_-/A_+ > 2$ . The accuracy of these calculations is not such that we could insist categorically on this. But such an interpretation appears very probable in connection with the fact that, in the study of a liquid-liquid system, where  $B_- \approx B_+$ <sup>[25]</sup>, the ratio  $A_-/A_+$  is close to 2.1. It is possible that the nonremovable asymmetry of the coexistence curves of all liquids also indicates the existence of such a break. It is likely that the only alternative to this point of view could be the complete inapplicability of the scaling theory to the liquid-vapor critical point<sup>1)</sup>.

Unfortunately, we do not have sufficient data to determine the asymptotic dependences  $C(t)$  along the various paths, and are forced to confine ourselves entirely to the reliable data of Table III, referring to the path  $\rho = \rho_C$ .

If we bear in mind all the circumstances lowering the precision of the determination of the index  $\alpha$ , and the slope of the curves in Fig. 7, we can assert that, with our accuracy,  $\alpha^* = \alpha'$ , and the indices of argon and ethane do not differ.

Figures 5 and 9 show the applicability of Eqs. (1) and (2) in a temperature region  $T < T_C$  so wide that the deviations from these equations seem more likely to be caused by the approach to the crystallization temperature than by too great a distance from  $T_C$ <sup>[26]</sup>. Thus, the range of possible applicability of the scaling theory is found to be extremely wide. Taking into account that crystallization of the liquid is already setting in at  $t \sim 0.5$ , we can say that almost the whole region of existence of the liquid is found to be the neighborhood of the critical point. In connection with this, the question of the possible range of applicability of the self-consistent field theory is important. Since for  $t \sim 0.5$  below  $T_C$  effects connected with the crystallization appear<sup>[26]</sup>, this question can be studied only for  $T > T_C$ .

For  $t \sim 1$ , the specific heat  $C_V$  of gases does not cease to depend on temperature even after subtraction of the specific heat  $C_{V0}$  of the ideal gas. This means that the self-consistent field theory, generally speaking,

<sup>1)</sup>It is possible that the transformation from the "isomorphous" variables  $\eta$ - $T$  to the experimental variables could be made on the basis of the scheme proposed in [23].

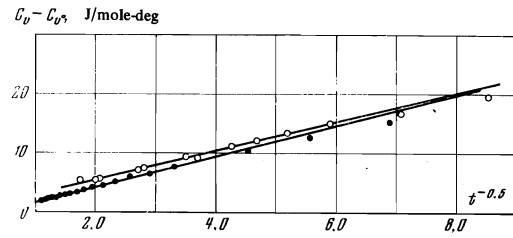


FIG. 10. Dependence of  $(C_V - C_{V0})$  on  $t^{-0.5}$  for nitrogen (O) and oxygen (O).

is inapplicable. However, in a narrow range of  $t$  close to unity, it may be suitable for the description of experiment, together with the first correction for the fluctuations (Ornstein-Zernike<sup>[27]</sup>) which gives a square-root dependence of the specific heat on temperature. Figure 10, using data on nitrogen<sup>[1]</sup> and oxygen<sup>[28]</sup>, shows that, in a narrow region, for comparatively large  $t$ ,  $C_V(t)$  approximates to a square-root dependence. This partly explains the tendency to overestimate the index which appears when the range of treatment of the data is broadened in the direction  $t > 10^{-2}$ . With regard to the underestimation of the index which appears for  $t < 10^{-4}$ , we cannot, unfortunately, state with confidence that it does not arise from the gradual appearance of the hydrostatic effect or of some other effect distorting the ideal conditions.

Thus, in the whole interval  $|t| < 1$ , we can expect the formulas of the scaling theory to be applicable, especially if we take into account not only the principal singular terms. Since this region completely encompasses the liquid state, it seems to us that it would be no exaggeration to regard the scaling theory as a sufficient basis for a new approach to the physics of the liquid state, at least for densities not too far from the critical density.

In conclusion, we thank M. A. Anisimov, E. E. Gorodetskiĭ, and M. Sh. Giterman for fruitful discussions of the results, and V. M. Bezmenov and G. A. Tarnovskii for help in the computer processing of the experimental data.

<sup>1</sup>A. V. Voronel', V. G. Gorbunova, Yu. R. Chashkin, and V. V. Shchekochikhina, Zh. Eksp. Teor. Fiz. 50, 897 (1966) [Sov. Phys.-JETP 23, 597 (1966)].

<sup>2</sup>A. V. Voronel' and Yu. R. Chashkin, Zh. Eksp. Teor. Fiz. 51, 394 (1966) [Sov. Phys.-JETP 24, 263 (1967)].

<sup>3</sup>C. Edwards, J. A. Lipa, and M. J. Buckingham, Phys. Rev. Lett. 20, 496 (1968).

<sup>4</sup>J. A. Lipa, C. Edwards, and M. J. Buckingham, Phys. Rev. Lett. 25, 1086 (1970).

<sup>5</sup>V. L. Pokrovskii, Usp. Fiz. Nauk 94, 127 (1968) [Sov. Phys.-Uspekhi 11, 66 (1968)].

<sup>6</sup>A. V. Voronel', S. R. Garber, and V. M. Mamnit-skiĭ, Zh. Eksp. Teor. Fiz. 55, 2017 (1968) [Sov. Phys.-JETP 28, 1065 (1969)].

<sup>7</sup>A. M. Bykov, A. V. Voronel', V. A. Smirnov, and V. V. Shchekochikhina, ZhETF Pis. Red. 13, 33 (1971) [JETP Lett. 13, 21 (1971)].

<sup>8</sup>A. V. Voronel', V. A. Smirnov, and Yu. R. Chashkin, ZhETF Pis. Red. 9, 387 (1969) [JETP Lett. 9, 229 (1969)].



- <sup>9</sup>A. V. Voronel' and Yu. R. Chashkin, *Izmeritel'naya Tekhnika (Measurement Techniques)* **2**, 77 (1967).
- <sup>10</sup>E. I. Ponomarenko and N. G. Shmakov, *Prib. Tekh. Eksp. No. 6*, 190 (1970).
- <sup>11</sup>A. T. Berestov and S. P. Malysenko, *Zh. Eksp. Teor. Fiz.* **58**, 2090 (1970) [*Sov. Phys.-JETP* **31**, 1127 (1970)].
- <sup>12</sup>Yu. R. Chashkin, A. V. Voronel', V. A. Smirnov, and V. G. Gorbunova, *Zh. Eksp. Teor. Fiz.* **52**, 112 (1967) [*Sov. Phys.-JETP* **25**, 72 (1967)].
- <sup>13</sup>P. C. Hohenberg and M. Barmatz, *Phys. Rev.* **A6**, 289 (1972).
- <sup>14</sup>M. Sh. Gitterman and V. A. Shteinberg, *Teplofizika Vysokikh Temperatur*, No. 3, 1972.
- <sup>15</sup>Yu. V. Tsekhanskaya, Z. A. Polyakova, and T. M. Kozlovskaya, *Zh. Fiz. Khim.* **41**, 501 (1967) [*Russ. J. Phys. Chem.* **41**, 253 (1967)].
- <sup>16</sup>L. A. Makarevich and E. S. Sokolova, *ZhETF Pis. Red.* **4**, 409 (1966) [*JETP Lett.* **4**, 276 (1966)].
- <sup>17</sup>Yu. R. Chashkin, V. A. Smirnov, and A. V. Voronel', *Teplofizicheskie svoistva veshchestv i materialov (Thermophysical Properties of Substances and Materials) (Bureau of Standards, M.)* no. 2, 139 (1970).
- <sup>18</sup>C. N. Yang and C. P. Yang, *Phys. Rev. Lett.* **13**, 303 (1964).
- <sup>19</sup>M. Ya. Azbel', A. V. Voronel', and M. Sh. Gitterman, *Zh. Eksp. Teor. Fiz.* **46**, 673 (1963) [*Sov. Phys.-JETP* **19**, 457 (1964)].
- <sup>20</sup>P. Schofield, J. D. Litster, and J. T. Ho, *Phys. Rev. Lett.* **23**, 1098 (1969).
- <sup>21</sup>G. Ahlers, *Phys. Rev. Lett.* **23**, 464 (1969).
- <sup>22</sup>G. Ahlers, *Phys. Rev. Lett.* **21**, 1159 (1968).
- <sup>23</sup>M. A. Anisimov, A. V. Voronel', and E. E. Gorodetskiĭ, *Zh. Eksp. Teor. Fiz.* **60**, 1117 (1971) [*Sov. Phys.-JETP* **33**, 605 (1971)].
- <sup>24</sup>N. D. Mermin and J. J. Rehr, *Phys. Rev. Lett.* **26**, 1155 (1971).
- <sup>25</sup>M. A. Anisimov, A. V. Voronel', and T. M. Ovodova, *Zh. Eksp. Teor. Fiz.* **61**, 1092 (1971) [*Sov. Phys.-JETP* **34**, 583 (1972)].
- <sup>26</sup>A. V. Voronel', *ZhETF Pis. Red.* **14**, 263 (1971) [*JETP Lett.* **14**, 174 (1971)].
- <sup>27</sup>V. G. Vaks, A. I. Larkin, and S. A. Pikin, *Zh. Eksp. Teor. Fiz.* **51**, 361 (1966) [*Sov. Phys.-JETP* **24**, 240 (1967)].
- <sup>28</sup>R. D. Goodwin and L. A. Weber, *J. Res. Nat. Bur. Stand.* **73A**, 1 (1969).

Translated by P. J. Shepherd

102